

# CHARACTERIZATION OF BACKSCATTER BY SURFACE FEATURES IN L-BAND ACTIVE MICROWAVE REMOTE SENSING OF SOIL MOISTURE

Narendra N. Das<sup>a</sup>, Binayak P. Mohanty<sup>a</sup>, Eni G. Njoku

<sup>a</sup>Department of Biological and Agricultural Engineering, Texas A&M University, Texas, United States

<sup>b</sup>Jet Propulsion Laboratory, Caltech, Pasadena, California, United States

## ABSTRACT

Satellite-based remote sensing of soil moisture is generally conducted with active (radar) and passive (radiometer) microwave measurements. During active microwave remote sensing the backscattering from the target i.e, the soil surface is adversely affected by the overlaying vegetation, consequently, sending degraded signal back to the radar sensor. This phenomena greatly compromise with the quality of soil moisture measurements. The proposed research presents an algorithm that averts usage of theoretical and empirical backscattering models. The algorithm uses Soil-Vegetation-Atmosphere-Transfer model for soil moisture estimation that is used to quantify the backscattering components of radar signals. The algorithm has simple and valid assumptions that convert the total radar backscattering equations for a particular temporal scale into a set of simple linear systems. The algorithm reasonably estimates the stochastic surface roughness and vegetation backscattering components.

## 1. INTRODUCTION

Microwave remote sensing is considered suitable to quantitatively measure soil moisture under variety of soil, topographic and vegetation conditions, and particularly the earth's atmosphere is relatively transparent to microwave. Microwave (active/passive) remote sensing of soil moisture, however, remains an active area of investigation because of its dependency on variety of geophysical parameters (e.g., precipitation, soil type, topography, and vegetation) and sensor configuration (system parameters: frequency, incident angle, and polarization), and due to coarse spatial resolution of remote sensor that mask the underlying ground heterogeneity.

Satellite-based passive microwave remote sensing is not adequate to meet the finer scale spatial resolution requirement for soil moisture in watershed, catchment, and field scale applications with the available configurations and associated limitations in terms of coarse resolution. The only satellite-based sensor that can meet the spatial resolution requirement for watershed and finer scale management is by using active microwave remote sensing techniques. *Dobson and Ulaby* [1] in their study showed that using active microwave (radar) soil moisture (with  $\pm 3.5\%$  vol/vol error) for spatial resolutions down to 1 km may be retrieved for soil surfaces with vegetation cover shorter than 15 cm. In active microwave remote sensing, the radar backscattering from the soil surface is adversely affected by the presence of vegetation. This is due to increased volume scattering and attenuation of electromagnetic signal. The overall impact of vegetation, surface roughness, and topography on radar signals results significantly higher root mean square error (RMSE) for soil moisture retrieval

[1]. Studies have also demonstrated that SAR instruments at C-band measure soil moisture for bare soil with nearly 3-4% vol/vol retrieval error. However, with SAR C-band it is difficult to map soil moisture accurately from the soil surface covered with vegetation. Many studies examined backscattering from soil under different vegetation conditions at various frequencies in L-, C-, and X-band at cross and like polarizations, and reported that backscattering is better related to soil moisture only at L-band frequency.

At present, there is no operational L-band radar satellite system. The upcoming Soil Moisture Active Passive (SMAP) mission of National Aeronautic and Space Administration (NASA) is a pathfinder-class concept for global mapping of soil moisture. The SMAP will have onboard low-frequency L-band radiometer (1.42 GHz) and radar (1.26 GHz). It will have soil moisture product derived from  $\sim 40$  km resolution brightness temperature from the L-band radiometer and  $\sim 3$  km resolution backscattering coefficients from the L-band radar with a revisit period of 2-3 days. The radar on SMAP platform is of particular interest here because it will provide a new perspective of L-band radar backscattering from a satellite platform. The study proposes a simple algorithm for determining stochastic surface roughness using synthetic radar data. The study also characterizes L-band radar backscattering coefficients under variety of terrain characteristics and vegetation conditions.

## 2. MODELING ACTIVE MICROWAVE SENSING OF SURFACE SOIL MOISTURE

We hypothesize that a reliable spatio-temporal distribution of soil moisture is important for probabilistic characterization of backscatter by surface features in active microwave remote sensing. The SVAT model [2] used in the study incorporates Dobson's model that converts the modeled soil moisture to dielectric constant  $\epsilon$ . Geophysical parameters (e.g., NDVI, soil texture, surface roughness) characterizing the study domain and estimated  $\epsilon$  from SVAT modeling provided synthetic radar total backscatter. The radar backscatter for a vegetation-covered soil layer in both HH and VV polarizations is expressed as [3],

$$\sigma^t = \sigma^s \exp(-2\tau_v / \cos\theta) + \sigma^v + \sigma^{sv} \quad (1)$$

where  $\sigma^t$  represents the total radar scattering cross-section,  $\sigma^s$  is the scattering contribution of the soil surface modified by the two-way vegetation attenuation,  $\sigma^v$  is the scattering cross-section of the vegetation volume, and  $\sigma^{sv}$  represents the multiple scattering interaction between the soil and vegetation. Subsequently the terminology, vegetation backscattering and soil-vegetation backscattering are interchangeably used with volume scattering and surface-volume scattering, respectively.

In practice, theoretical and empirical models are used to model the scattering components  $\sigma^s$ ,  $\sigma^v$ , and  $\sigma^{sv}$ . In case of the above-ground biomass (vegetation) is lesser than 0.5 kg/m<sup>2</sup>, the second and third terms ( $\sigma^v$  and  $\sigma^{sv}$ ) on the right side in eq. (1) become negligibly small. At radar L-band, the soil surface backscatter  $\sigma^s$  can be modeled theoretically by Integral Equation Model (IEM). For a given radar configuration (i.e., wavelength, local incident angle and polarization), the IEM predicts the backscattering coefficient on a random surface depending on surface roughness (RMS height)  $s$  and its correlation length  $l$ , and the relative dielectric constant  $\epsilon$ . For bare soil, there is a general confidence using the IEM in predicting L-band co-polarized backscattering signals ( $\sigma_{VV}^s$  and  $\sigma_{HH}^s$ ) of a random rough surface. Studies have also shown that the results from IEM deviated when compared to truck-mounted scatterometer and SAR (airborne and spaceborne) measurements. The theoretical models like IEM can rarely invert data measured from natural environment because of restrictive assumptions made during their derivation. Well established alternative empirical methods are used in this study to circumvent the difficulties for modeling the backscattering signatures of bare surfaces. The empirical models for backscattering coefficient of bare soil  $\sigma_{VV}^s$  and  $\sigma_{HH}^s$  are derived from experimental data. *Dubois, et al.* [4] provide empirical expressions for  $\sigma_{VV}^s$  and  $\sigma_{HH}^s$  that is used in this study for the co-polarized backscatter,

$$\sigma_{HH}^s = 10^{-2.75} \frac{\cos^{1.5} \theta}{\sin^5 \theta} 10^{0.028\epsilon \tan \theta} (ks * \sin \theta)^{1.4} \lambda^{0.7} \quad (2)$$

$$\sigma_{VV}^s = 10^{-2.35} \frac{\cos^3 \theta}{\sin^3 \theta} 10^{0.046\epsilon \tan \theta} (ks * \sin \theta)^{1.1} \lambda^{0.7} \quad (3)$$

where,  $\theta$  is radar incidence angle,  $\lambda$  (cm) is the wavelength,  $k$  is the wave number,  $s$  is the surface RMS height, and  $\epsilon$  is the real part of the dielectric constant. The presence of vegetation biomass adds complexity and increase uncertainty in total radar backscattering. For radar backscatter modeling (unlike radiometric modeling) a uniform canopy assumption may not be adequate to describe the microwave-vegetation interactions. In this study, over the spatial extent of the 3-km radar footprints, the models for the co- and cross-polarized backscatter from vegetation represented as randomly orientated-structures are evaluated as [5].

Our numerical study uses a Soil-Vegetation-Atmosphere-Transfer model [2] for soil moisture/dielectric constant modeling in conjunction with empirical models for  $\sigma^s$ ,  $\sigma^v$ , and  $\sigma^{sv}$  to characterize the spatial and temporal variability of microwave backscattering components. This synthetic data obtained from eq. 1 is considered as the total backscattering received by the satellite-based radar and is the basis for the characterization of uncertainty in radar backscattering and proposed algorithm (Section 3).

### 3. A NEW ALGORITHM FOR ESTIMATING SURFACE ROUGHNESS AND VOLUME SCATTERING

Using the synthetic radar backscattering data, the study uses a new algorithm to determine the surface roughness and vegetation backscattering components as an alternative to using any of the aforementioned empirical models. In the proposed algorithm, the surface roughness parameter ( $s$ ) and the vegetation backscattering ( $\sigma^v$ ) are considered static for a small temporal scale (i.e., interstorm period). This is a reasonable assumption based on the growth/decay status of vegetation in natural environment and soil surface getting modified after precipitation events. Also the parameters such as  $s$  and  $\sigma^v$  are considered not very dynamic for pasture and herbaceous

fields for small temporal scale. The backscattering due to soil-vegetation interaction component ( $\sigma^{sv}$ ) is the most dynamic because along with vegetation it is greatly influenced by the temporal status of dielectric constant which is highly correlated to soil moisture evolution. Based on these assumptions and conditions, a new approach is proposed here for determining surface roughness and backscatter components. For co-polarized radar backscattering from a specific region for a particular day ( $x$ ) is given as

$$\sigma_x^t = \sigma_x^s(-2\tau_0/\cos\theta) + \sigma_x^v + \sigma_x^{sv} \quad (4)$$

where  $x = 1 \dots n$ , represents a daily timestep within an interstorm period  $T$ . In other words the system has  $n$  sets of equations. By solving the  $n$  sets of equations simultaneously eliminated  $\sigma^v$  from all the equations as that component is considered constant across  $T$ . The backscattering from the soil surface  $\sigma_x^s$  has two unknowns,  $\epsilon_x$  (dielectric constant for day  $x$ ) and  $s$  in all the  $n$  equations. To compute dielectric constant reliable soil moisture at compatible resolution is essential. The SVAT model provides reasonable distribution of state variable i.e., soil moisture at soil surface for ~3 km resolution. Subsequently Dobson's model relates soil moisture to equivalent dielectric constant. Now the system of  $n$  simultaneous equations comprise  $n+1$  unknowns (i.e.,  $s$ ,  $\sigma_1^{sv}, \dots, \sigma_n^{sv}$ ). To solve  $n$  simultaneous equations with  $n+1$  unknowns, we assumed  $\sigma_1^{sv} \approx \sigma_2^{sv}$ . The rationale of  $\sigma_1^{sv} \approx \sigma_2^{sv}$  is that at the start of interstorm period and due to wet condition of soil surface the probability of  $\sigma_1^{sv} \approx \sigma_2^{sv}$  is high. The assumption is even more appropriate for the region having high vegetation and also the region with soil texture having high percentage of clay fraction that retains high soil moisture. This assumption reduced the number of unknowns to  $n$ , leading to computation of  $s$ ,  $\sigma^v$ ,  $\sigma_1^{sv}, \dots, \sigma_n^{sv}$ , for the interstorm period. The algorithm applied to certain regions for continuous interstorm periods could help study the temporal evolution and statistical characteristics of surface roughness  $s$  with changing season, precipitation, vegetation growth and vegetation water content.

### 4. STUDY AREA AND DATA

The Red-Arkansas river basin (Fig. 1) is selected for this study due to presence of diverse geophysical characteristics (topography, soil type and vegetation). Three specific regions (Fig. 1) are selected as focus areas: i) Northwestern mountainous region (50,000 km<sup>2</sup>), with elevation more than 1200 m from the sea level and having low vegetation (LAI between 0 and 1.2 m<sup>2</sup>/m<sup>2</sup>). ii) Central plains of farmlands/grasslands (38,000 km<sup>2</sup>) with moderate elevation between 150 m and 500 m of rolling topography and having highly variable LAI between 1 and 5 m<sup>2</sup>/m<sup>2</sup>, reaching its maximum during the summer months. iii) Eastern plains, of low lying (elevation: 40 to 100 m) eastern region (38,000 km<sup>2</sup>). The landcover has moderate to high LAI of nearly 1 to 6 m<sup>2</sup>/m<sup>2</sup>. The other relevant datasets used in the study are summarized below:

Soil: The requisite soil parameters (e.g., %sand, %clay, bulk density and saturated hydraulic conductivity) data were derived from CONUS-SOIL (<http://www.soilinfo.psu.edu/>) dataset.

NDVI and LAI: MODIS derived 16-day composite data of NDVI and LAI at ~1 km spatial resolution were obtained and resampled to ~3 km for the study.

Precipitation: Quality-controlled ~4 km precipitation data based on multi-sensor (radar WSR-88D and rain gauge) estimates from National Weather Service (NWS) River Forecast Centers (RFCs) and resampled to ~3 km (matching SMAP-based L-band radar spatial resolution) is used for the study.

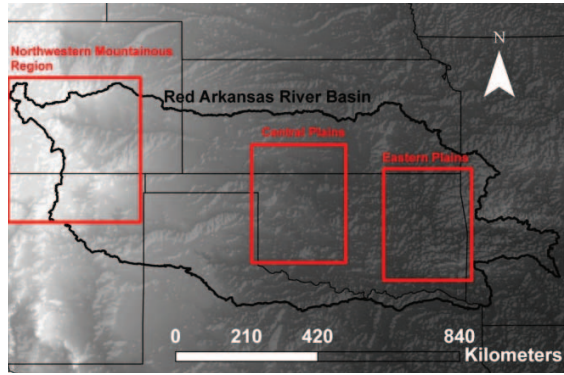


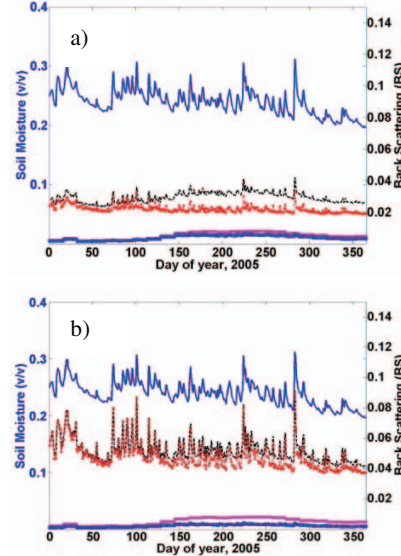
Figure 1. Red-Arkansas River Basin with highlighted region showing three focus study area: a) the Northwestern Mountainous Region, b) the Central Plains, and c) the Eastern Plains.

## 5. RESULT AND DISCUSSIONS

SVAT modeling based on a distributed modeling framework [2] that have an ensemble of appropriate boundary conditions and scaled parameters was used to simulate soil moisture, soil temperature, and evapotranspiration in the Red-Arkansas river basin at a spatial resolution of  $\sim 3$  km for the year 2005. Arbitrarily selected random error of 0-10% was introduced in the soil moisture values and the parameters (surface roughness, tree fraction, albedo, and vegetation opacity). The random error of 0-10% was to make the synthetic backscattering data more representative of chaos in the backscattering dynamics. The surface (i.e., top 5 cm) soil moisture from the simulation was used to compute total radar backscattering and its individual components (soil, vegetation, and soil-vegetation interaction). Mainly, backscattering based on HH/VV polarization was considered as the HV/VH cross polarization return was usually weaker than the like polarized return. Results presented in the subsequently are based on the average values of backscattering components within the study regions (i.e., the Northwestern mountainous region, the Central plains, and the Eastern plains). For brevity, the results of Northwestern Mountainous Region are discussed in detail.

The Northwestern Mountainous Region is dominated by rugged topography and mountains, has low yearly average NDVI, and low average ambient temperature. The average soil moisture of this region is nearly 0.25 (v/v) with occasional spikes due to precipitation events. As expected, the backscattering at HH/VV polarization ( $\sigma_{HH}^s, \sigma_{VV}^s$ ) from soil corresponds with soil moisture (Fig. 2a-b), although the variation and correspondence of  $\sigma_{HH}^s$  (Fig. 2a) with soil moisture evolution is not as pronounced as  $\sigma_{VV}^s$  (Fig. 2b), and is relatively constant throughout the year. Numerous investigations (e.g., [6]) have also shown that backscattering from soil having VV polarization ( $\sigma_{VV}^s$ ) is more sensitive to soil moisture than  $\sigma_{HH}^s$ . The time series of HH total backscattering ( $\sigma_{HH}^t$ ) (Fig. 2a) makes a hump in the middle of the year due to increase in NDVI value that ultimately increase the HH vegetation ( $\sigma_{HH}^v$ ) and soil-vegetation backscattering ( $\sigma_{HH}^{sv}$ ) components. However, this phenomenon is not visible with VV polarization (Fig. 2b). It mainly resulted from the surface-volume (soil-vegetation) interaction term that has the characteristics  $\sigma_{HH}^{sv} > \sigma_{VV}^{sv}$ . For this region the overall trend in  $\sigma_{HH}^t$  could be attributed to the trends in  $\sigma_{HH}^v$  and  $\sigma_{HH}^{sv}$  backscattering components.

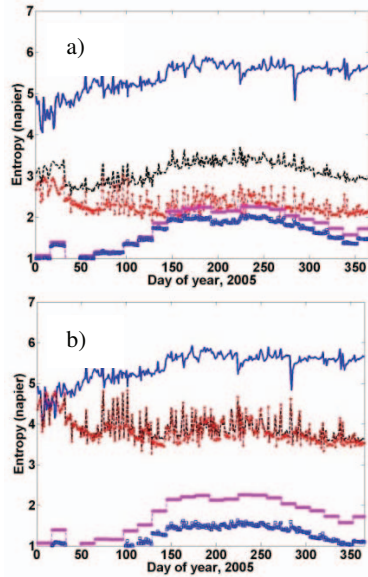
Figure 2. Mean soil moisture and mean backscattering components of the Northwestern Mountainous Region: a) at HH polarization, and b) at VV polarization.



To capture chaos and randomness in radar backscattering in diverse hydro-climatic, terrain, and vegetation, Shannon entropy is used. Shannon entropy takes on a maximum value when the probability distribution is uniform without any deflection, and it reduces to zero when a particular value of the variable occurs with probability of one. Figure 3 highlights the uncertainty in

terms of entropy associated with soil moisture and backscattering components for the Northwestern Mountainous Region. The difference in entropy values is distinct when the  $\sigma_{HH}^s$  and  $\sigma_{VV}^s$  components are compared. This property of  $\sigma_{VV}^s$  component having high entropy values is attributed to the higher sensitivity to change in dielectric constant of soil medium with respect to change in soil moisture. In contrast, high entropy is not visible in the  $\sigma_{HH}^s$  component (Fig. 3a). The entropy of  $\sigma_{HH}^s$  component for this region is relatively consistent for the whole study period. Another noticeable feature in Fig. 3a-b is the contribution of entropy of vegetation and soil-vegetation backscattering components in the overall response of HH/VV total backscattering ( $\sigma_{HH}^t, \sigma_{VV}^t$ ) entropy. In case of HH polarization, the first harmonic of  $\sigma_{HH}^t$  entropy corresponds to the entropy of  $\sigma_{HH}^v$  and  $\sigma_{HH}^{sv}$  components, and the higher harmonic responds to the  $\sigma_{HH}^s$  component. However, the entropy of  $\sigma_{VV}^t$  is almost unaffected by the entropy of  $\sigma_{VV}^s$  and  $\sigma_{VV}^{sv}$  component. The entropy of  $\sigma_{VV}^t$  only responds to the entropy of  $\sigma_{VV}^s$  component. This indicates that with sparse vegetation, the scattering in L-band at VV ( $\sigma_{VV}^s$ ) polarization is dominated by the underlying surface and not by the vegetation and HH ( $\sigma_{HH}^t$ ) polarization is influenced by the overlaying vegetation. The mean plots in Fig. 2 shows the influence of the vegetation on total backscattering, but the entropy plot distinctly illustrates the effects in Fig. 3. The findings emphasize the dependence of  $\sigma_{HH}^t$  on vegetation (i.e., NDVI) as an important index for algorithm development for the high elevation mountainous region. Similar analysis conducted for the Central Plains and the Eastern Plains show backscattering at HH polarization capture more variability (high entropy) in  $\sigma_{HH}^v$  and  $\sigma_{HH}^{sv}$  components. In the Eastern Plains, due to high amount of vegetation the entropy of  $\sigma_{VV}^s$  is also quite significant and is not seen in other region of the study area.

Figure 3. Entropy of soil moisture and backscattering components of the Northwestern Mountainous Region: a) at HH polarization, b) at VV polarization, and c) at HV polarization.



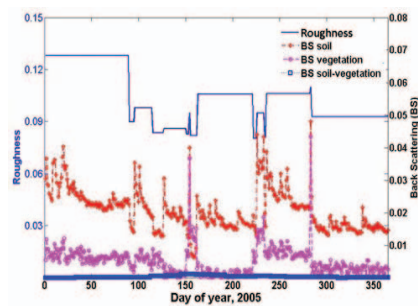
### 5.1. Estimation of Surface Roughness and Volume Scattering

The new algorithm proposed here (Section 3) exploits the radar backscattering components for determining certain geophysical parameters. As discussed in the above sections, the L-band HH polarization ( $\sigma_{HH}^t$ ) is most sensitive to the presence of vegetation which influence the roughness. Therefore, the HH polarization is used to evaluate  $s$ . The algorithm uses the

synthetic  $\sigma_{HH}^t$ , surface average soil moisture (~5 cm), soil temperature, and precipitation data to estimate the surface roughness and vegetation backscattering. The assumptions and stochasticity in the algorithm introduce uncertainty in derived surface roughness estimates. The derived values of surface roughness depend on the inter-storm period, dielectric model and the assumption of static vegetation within the inter-storm period. In the study region, the validity of assumptions stands a better likelihood during spring and summer months, where the inter-storm periods are small. The smaller inter-storm period can capture the dynamics of variable surface roughness. However, for extended inter-storm events, the cumulative errors of algorithm assumptions (static vegetation within the inter-storm) and errors in the model and data may lead to an inferior estimate of surface roughness. For the Northwestern Mountainous Region, a randomly selected pixel, Fig. 4 shows the derived surface roughness and vegetation backscattering components. The result shows that the surface roughness from the algorithm is very similar to the values used in calculating the synthetic radar backscattering data. The surface roughness exhibits variability during spring and summer months, and are more reliable estimate due to shorter interstorm period. The algorithm-estimated vegetation backscattering component shows consistency with respect to derived surface roughness, sparse vegetation and soil backscattering component for the pixel. However, the derived vegetation backscattering parameter shows nearly 25% absolute errors, when compared to synthetic data for the particular pixel. Similarly, other randomly selected pixels show absolute error ranging 20-30%. The errors in estimated vegetation backscattering are expected and are within reasonable limits considering the simplified assumptions used in the algorithm. The algorithm evaluated less variability and consistency in surface roughness parameter for the Central Plains that agrees with the existing ground conditions. The average surface roughness is slightly overestimated by 10%, when compared to the value used for calculating the synthetic data. The estimated vegetation backscattering for the region has absolute errors ranging between 23% and 36%. For the Eastern plains, the maximum surface roughness is observed that is consistent to the presence of dense vegetation that imparts to this attribute. However, the surface roughness is overestimated by nearly 20%. For the Eastern plains,

an absolute error ranging between 25% and 35% is obtained for estimated vegetation backscattering. The algorithm performed reasonably well in approximating surface roughness of the study areas. In case of estimation of vegetation backscattering, the algorithm produced considerable errors. The major portion of errors in vegetation backscattering is the consequence of the mismatch of inter-storm period and NDVI 16 days composite data. However, with the future availability of satellite-based radar data at L-band, the problem of high error in vegetation backscattering is expected to reduce significantly by including the co-registered remote sensing of vegetation water content in the algorithm.

Figure 4. Algorithm-based derived surface roughness and combined vegetation backscattering of the Northwestern Mountainous Region.



### 6. CONCLUSION

An algorithm using SVAT model and radar backscattering data is presented to derive stochastic surface-roughness and volume scattering by vegetation. The results were

promising for estimation of surface-roughness. However, further studies and realistic radar data is required to reduce the errors in estimation of vegetation volume backscattering. The work advances our understanding in active microwave remote sensing of soil moisture with region specific characterizations of backscattering components. The entropy-based characterization scheme of backscattering dynamics for variety of soil, topographic and vegetation conditions will help improve the radar-based soil moisture retrieval for upcoming SMAP mission of NASA.

### 7. REFERENCES

- [1] M. C. Dobson and F. T. Ulaby, "Active microwave soil moisture research," *IEEE Transactions on Geoscience and Remote Sensing*, vol. GE-24, pp. 23–36, 1986.
- [2] N. N. Das, B. P. Mohanty, M. H. Cosh, and T. J. Jackson, "Modeling and Assimilation of Root Zone Soil Moisture Using Remote Sensing Observations in Walnut Gulch Watershed During SMEX04," *Remote Sensing of Environment*, vol. 112, pp. 415-429, 2008.
- [3] F. T. Ulaby, P. C. Dubois, and J. van Zyl, "Radar mapping of surface soil moisture," *Journal of Hydrology*, vol. 184, pp. 57-84, 1996.
- [4] P. C. Dubois, J. Vanzyl, and T. Engman, "Measuring Soil-Moisture with Imaging Radars," *IEEE Transactions on Geoscience and Remote Sensing*, vol. 33, pp. 915-926, 1995.
- [5] F. T. Ulaby, R. K. Moore, and A. K. Fung, *Microwave remote sensing active and passive* vol. 3. Norwood, MA: Artech House, Inc., 1986.
- [6] E. G. Njoku, W. J. Wilson, S. H. Yueh, S. J. Dinardo, F. K. Li, T. J. Jackson, V. Lakshmi, and J. Bolten, "Observations of soil moisture using a passive and active low-frequency microwave airborne sensor during SGP99," *IEEE Transactions on Geoscience and Remote Sensing*, vol. 40, pp. 2659-2673, 2002.